Bull. Inst. Chem. Res., Kyoto Univ., Vol. 63, No. 3, 1985

Improved Evaluation of Electrical Phase Parameters in a Dielectric Theory for Concentrated Suspensions of Spherical Particles

Tetsuya HANAI, Katsuhisa SEKINE and Naokazu KOIZUMI*

Received June 20, 1985

An improved method is proposed to find a physicochemically significant solution of the equation which was presented in a previous paper [*Bull. Inst. Chem. Res., Kyoto Univ.*, **55**. 376 (1977)] to evaluate electrical conductivity of the continuous phase in a concentrated suspension of spherical particles. An existing domain of the complex permittivity of the suspension was made clear in a permittivity-conductivity plane with mathematical formulas as well as with graphic representation. As a consequence, the searching scheme for the root was refined so as to attain to the correct root of the equation straightway. Some numerical examples are shown to confirm the validity of the improved method.

KEY WORDS: Concentrated suspension/ Dielectric relaxation/ Electirical conductivity/ Interfacial polarization/ Maxwell-Wagner relaxation/ Permittivity/

I. INTRODUCTION

It was reported by a number of workers[1-3] that coarsely dispersed systems such as emulsions and suspensions showed remarkable dielectric relaxations, which were understood to be caused by the interfacial polarization due to their diphasic structure.

Such dielectric relaxations caused by interfacial polarization for suspensions of spherical particles were first pointed out by Maxwell,[4] having been afterwards formulated by Wagner[5] in a form convenient for the comparison with experiments. Since closer consideration revealed that Wagner's equation was in poor agreement with expermients at higher concentrations of the suspended particles, Hanai[6,7] proposed a theoretical equation which is expected to be applicable up to higher concentrations.

On the basis of Hanai's equation, a systematic method[8] was proposed to calculate the relative permittivity, the electrical conductivity, and the concentration of the suspended particles by use of the observed data on dielectric relaxation caused by a diphasic structure of spherical disperse systems. The method proposed, however, was not necessarily successful in evaluating the electrical conductivity of the suspended particles in such a way that the computer searching for the solution of an equation in the theory sometimes takes hold of a false root.

In the present paper, an effectual method is proposed to find a correct root of the equation. Several examples are illustrated to show merits of the proposed method on computer searching for the correct roots of the equation.

* 花井哲也, 関根克尚, 小泉直一: Laboratory of Dielectrics, Institute for Chemical Research, Kyoto University, Uji, Kyoto 611.

II EQUATIONS FOR CONCENTRATED DISPERSE SYSTEMS OF SPHERICAL PARTICLES

In order to make clear the circumstances in question, we shall summarize the equations used.[8)]

For a concentrated disperse system of spherical particles with a complex permittivity ε_i^* in a continuous medium with a complex permittivity ε_a^*, Hanai derived the following equation for the complex permittivity ε^* of the whole system:

$$\frac{\varepsilon^*-\varepsilon_i^*}{\varepsilon_a^*-\varepsilon_i^*}\left(\frac{\varepsilon_a^*}{\varepsilon^*}\right)^{1/3}=1-\phi, \tag{1}$$

where ϕ is the volume fraction of the dispersed particles. The complex permittivities ε^*, ε_a^* and ε_i^* are each defined by the following equations:

$$\varepsilon^*=\varepsilon-j\frac{\kappa}{2\pi f\epsilon_v}, \tag{2}$$

and

$$\varepsilon_a^*=\varepsilon_a-j\frac{\kappa_a}{2\pi f\epsilon_v}, \tag{3}$$

and

$$\varepsilon_i^*=\varepsilon_i-j\frac{\kappa_i}{2\pi f\epsilon_v}, \tag{4}$$

where j is $\sqrt{-1}$, f the frequency, ε the relative permittivity, κ the electrical conductivity and ϵ_v the permittivity of free space. The subscripts a and i refer to the continuous medium and the suspended particles, respectively.

The limiting values of ε and κ at high (subscript h) and low (l) frequencies are given by

$$\frac{\varepsilon_h-\varepsilon_i}{\varepsilon_a-\varepsilon_i}\left(\frac{\varepsilon_a}{\varepsilon_h}\right)^{1/3}=1-\phi, \tag{5}$$

$$\varepsilon_l\left(\frac{3}{\kappa_l-\kappa_i}-\frac{1}{\kappa_l}\right)=3\left(\frac{\varepsilon_a-\varepsilon_i}{\kappa_a-\kappa_i}+\frac{\varepsilon_i}{\kappa_l-\kappa_i}\right)-\frac{\varepsilon_a}{\kappa_a}, \tag{6}$$

$$\kappa_h\left(\frac{3}{\varepsilon_h-\varepsilon_i}-\frac{1}{\varepsilon_h}\right)=3\left(\frac{\kappa_a-\kappa_i}{\varepsilon_a-\varepsilon_i}+\frac{\kappa_i}{\varepsilon_h-\varepsilon_i}\right)-\frac{\kappa_a}{\varepsilon_a}, \tag{7}$$

and

$$\frac{\kappa_l-\kappa_i}{\kappa_a-\kappa_i}\left(\frac{\kappa_a}{\kappa_l}\right)^{1/3}=1-\phi. \tag{8}$$

Provided that ε_a, ε_h, ε_l, κ_h and κ_l are given from the observed data, we can obtain the values of κ_a by means of computer searching for the root of the following equation which was derived from Eqs. 5-8:

$$J(\kappa_a)=[3-(2+\frac{\varepsilon_a}{\varepsilon_h})C](1-DC)\kappa_h$$
$$-3[(1-C)\kappa_l+(1-D)C\kappa_a](1-C)$$
$$+(1-\frac{\varepsilon_h}{\varepsilon_a})(1-DC)C\kappa_a=0, \tag{9}$$

where

$$C=\frac{-Q-\sqrt{Q^2-4PR}}{2P}, \tag{10}$$

$$P=(2+\frac{\kappa_a}{\kappa_l})D\varepsilon_l-3[D\varepsilon_h+(1-D)\varepsilon_a]D+(\frac{\kappa_l}{\kappa_a}-1)D\varepsilon_a, \tag{11}$$

$$Q=3[2D\varepsilon_h+(1-D)\varepsilon_a]-[(2+\frac{\kappa_a}{\kappa_l})D+3]\varepsilon_l-(\frac{\kappa_l}{\kappa_a}-1)D\varepsilon_a, \tag{12}$$

$$R=3(\varepsilon_l-\varepsilon_h), \tag{13}$$

$$D=(\frac{\varepsilon_a\kappa_l}{\varepsilon_h\kappa_a})^{1/3}. \tag{14}$$

Using the values of κ_a thus obtained, values of Φ, ε_i and κ_i are calculated from the following equations in sequence:

$$\Phi=1-C(\frac{\varepsilon_a}{\varepsilon_h})^{1/3}, \tag{15}$$

$$\varepsilon_i=\frac{\varepsilon_h-C\varepsilon_a}{1-C}, \tag{16}$$

and

$$\kappa_i=\frac{\kappa_l-DC\kappa_a}{1-DC}. \tag{17}$$

According to the remarks shown in Appendices of the previous paper,[8] the computer searching for the root of Eq. 9 should be proceeded from κ_l toward the lower values of κ_a when $\kappa_a<\kappa_l$. If $\kappa_l<\kappa_a$, then the searching should be proceeded from κ_l toward the higher values of κ_a. After several trials of numerical calculations, it turned out incomplete to perform the above computer searching.

An improved computer searching is proposed on the basis of the discussion developed in the succeeding sections.

III. GRAPHIC EXPLANATION CONCERNING THE LOCATION OF ε^* ON THE $\varepsilon-\kappa$ PLANE

For the purpose of discussing the dielectric relaxation caused by the diphasic structure, the representation of ε^*(abscissa ε, ordinate κ) on an $\varepsilon-\kappa$ plane is more comprehensible and convenient as compared with the conventional plots on $\varepsilon-\varepsilon''$ planes.

In dielectric relaxation phenomena, the relative permittivity $\varepsilon(f)$ is a monotonically

decreasing function with increasing frequency, the conductivity $\kappa(f)$ being a monotonically increasing function —— that is, $\varepsilon_l > \varepsilon(f) > \varepsilon_h$ and $\kappa_l < \kappa(f) < \kappa_h$. In order to understand the behavior of $\varepsilon^*(\varepsilon(f), \kappa(f))$ on the $\varepsilon-\kappa$ plane, it is necessary to elucidate the locations of ε_l, ε_h, κ_l and κ_h first, and then those of $\varepsilon(f)$ and $\kappa(f)$.

For concentrated disperse systems of spherical particles in a type of $\kappa_i/\varepsilon_i > \kappa_a/\varepsilon_a$, the values of ε_l, ε_h, κ_l and κ_h were calculated from Eqs. 5-8 for different values of ε_a^* $(\varepsilon_a, \kappa_a)$ and Φ under a fixed $\varepsilon_i^*(\varepsilon_i, \kappa_i)$. The results are shown in Fig. 1, where the solid curves denote the loci of ε_l^* and the dashed curves those of ε_h^*. For concentrated disperse systems in a type of $\kappa_i/\varepsilon_i < \kappa_a/\varepsilon_a$, similar calculation was carried out, the results being shown in Fig. 2. As readily seen in Figs. 1 and 2, all the loci of ε_l^* and ε_h^* are located in a domain bounded by two straight lines $\overline{O\varepsilon_a^*}$ and $\overline{O\varepsilon_i^*}$.

Next, values of $\varepsilon(f)$ and $\kappa(f)$ or the frequency dependence was calculated from Eqs. 1-4 for an example shown in Fig. 1: $\varepsilon_a^*(\varepsilon_a=320,\ \kappa_a=8\ \mu\text{S cm}^{-1})$ and $\Phi=0.6$. The results are shown in Fig. 3. Similar calculation was carried out for an example shown in Fig. 2: $\varepsilon_i^*(\varepsilon_i=320,\ \kappa_i=8\ \mu\text{S cm}^{-1})$ and $\Phi=0.6$. The results are shown in Fig. 4. In these Figures 3 and 4, the values of ε and κ start from a point $L(\varepsilon_l, \kappa_l)$ at low frequencies, then proceed on the solid curves, finally reach a point $H(\varepsilon_h, \kappa_h)$ at high frequencies. The broken lines denote the loci of points L, the dotted broken lines the loci of points H.

We shall consider rectangles HMLN in Figs. 3 and 4. Points M and N are the locations of a complex numbers $\varepsilon_M^*(\varepsilon_h, \kappa_l)$ and $\varepsilon_N^*(\varepsilon_l, \kappa_h)$, respectively.

As readily seen in Figs. 3 and 4, the following inequalities seem to hold:

$$\frac{\kappa_a}{\varepsilon_a} < \frac{\kappa_l}{\varepsilon_l} < \left\{ \frac{\kappa_l}{\varepsilon_h},\ \frac{\kappa(f)}{\varepsilon(f)} \right\} < \frac{\kappa_h}{\varepsilon_h} < \frac{\kappa_i}{\varepsilon_i} \quad \text{in Fig. 3,} \tag{18}$$

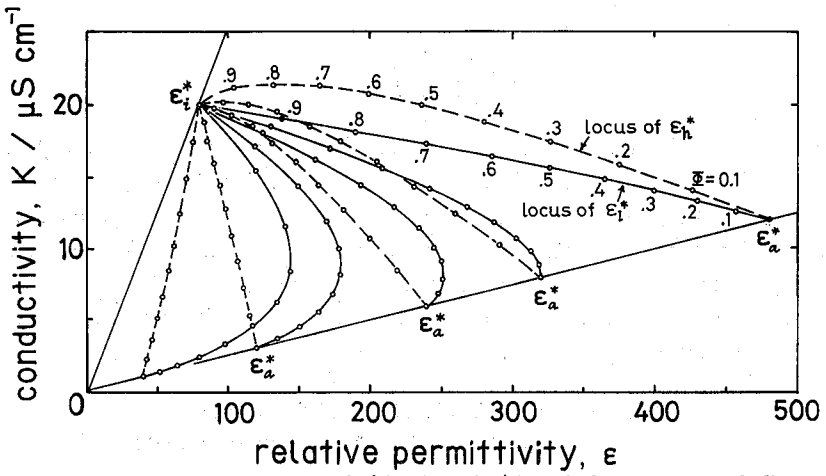

Fig. 1. Location on the $\varepsilon-\kappa$ plane of $\varepsilon_l^*(\varepsilon_l, \kappa_l)$ and $\varepsilon_h^*(\varepsilon_h, \kappa_h)$ for concentrated disperse systems of spherical particles in a type of $\kappa_i/\varepsilon_i > \kappa_a/\varepsilon_a$(W/O).
The solid curves show the loci of ε_l^*, and the dashed curves denote the loci of ε_h^* for varied concentrations Φ under a fixed $\varepsilon_i^*(\varepsilon_i, \kappa_i)$ and some of $\varepsilon_a^*(\varepsilon_a, \kappa_a)$.

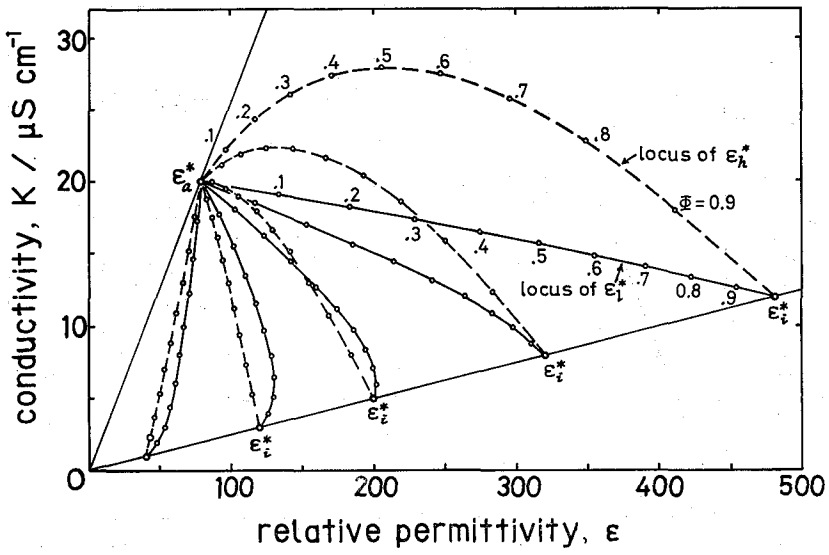

Fig. 2. Location on the $\varepsilon-\kappa$ plane of $\varepsilon_l^*(\varepsilon_l, \kappa_l)$ and $\varepsilon_h^*(\varepsilon_h, \kappa_h)$ for concentrated disperse systems of spherical particles in a type of $\kappa_i/\varepsilon_i < \kappa_a/\varepsilon_a$ (O/W). The solid curves show the loci of ε_l^*, and the dashed curves denote the loci of ε_h^* for varied concentrations Φ under a fixed ε_a^* $(\varepsilon_a, \kappa_a)$ and some of $\varepsilon_i^*(\varepsilon_i, \kappa_i)$.

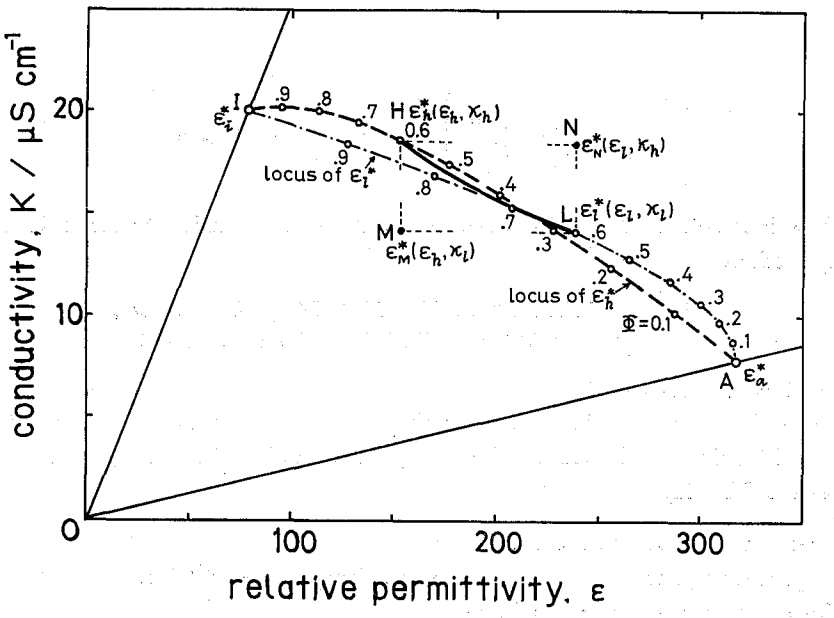

Fig. 3. Location of the $\varepsilon-\kappa$ plane of ε_l^*, ε_h^* and $\varepsilon^*(f)$, $\varepsilon_a=320$, $\kappa_a=8\ \mu$S cm^{-1}, $\varepsilon_i=80$, $\kappa_i=20\ \mu$S cm^{-1}.
The solid curve shows the locus of $\varepsilon^*(\varepsilon(f), \kappa(f))$ for a fixed concentration $\Phi=0.6$, and the dotted broken curve denotes the locus of ε_l^*, the dashed curve the locus of ε_h^*.

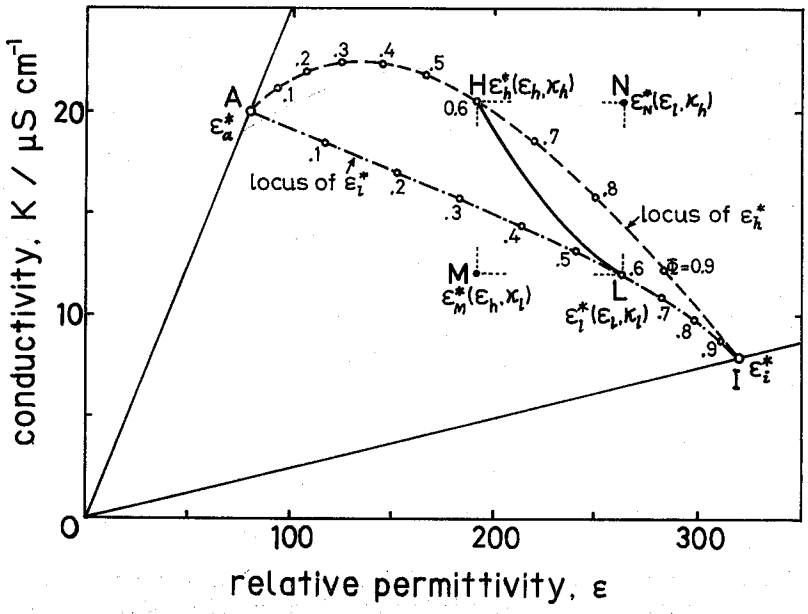

Fig. 4. Location on the $\varepsilon-\kappa$ plane of ε_l^*, ε_h^* and $\varepsilon^*(f)$. $\varepsilon_a=80$, $\kappa_a=20\ \mu$S cm^{-1}, $\varepsilon_i=320$, $\kappa_i=8\ \mu$S cm^{-1}.
The solid curve shows the locus of $\varepsilon^*(\varepsilon(f), \kappa(f))$ for a fixed concentration $\Phi=0.6$, and the chain dotted broken curve denotes the locus of ε_l^*, the dashed curve the locus of ε_h^*.

and

$$\frac{\kappa_i}{\varepsilon_i} < \frac{\kappa_l}{\varepsilon_l} < \left\{ \frac{\kappa_l}{\varepsilon_h},\ \frac{\kappa(f)}{\varepsilon(f)} \right\} < \frac{\kappa_h}{\varepsilon_h} < \frac{\kappa_a}{\varepsilon_a} \quad \text{in Fig. 4.} \tag{19}$$

These inequalities 18 and 19 will be derived by mathematical formulas in the succeeding sections.

IV. RESTRICTION OF EXISTING DOMAINS OF κ_a/ε_a BY MEANS OF MATHEMATICAL FORMULAS

4.1 Definition of Emulsion Type

It is well known that dielectric relaxations cease to be observable when $\kappa_a/\varepsilon_a=\kappa_i/\varepsilon_i$. From a viewpoint of dielectric relaxations, therefore, it is natural to define emulsion types as the following:

a. water-in-oil (W/O) type emulsions
b. homogeneous solutions
c. oil-in-water (O/W) type emulsions

} according as $T \equiv \frac{\varepsilon_a \kappa_i}{\kappa_a \varepsilon_i} \gtrless 1$. (20)

A new function S is further introduced as

$$S \equiv \frac{T}{D^3} = \frac{\varepsilon_h \kappa_i}{\kappa_l \varepsilon_i}. \tag{21}$$

4.2 Existing Domain of κ_l/ε_h

For cases of physical significance, ε_h and κ_l given by Eqs. 5 and 8 are monotonic functions with respect to Φ, being restricted as follows:

either $$0<\varepsilon_a<\varepsilon_h<\varepsilon_i, \tag{22}$$

or $$\varepsilon_a>\varepsilon_h>\varepsilon_i>0, \tag{23}$$

and

either $$0<\kappa_a<\kappa_l<\kappa_i, \tag{24}$$

or $$\kappa_a>\kappa_l>\kappa_i>0. \tag{25}$$

Therefore we have

$$0<\frac{\varepsilon_h-\varepsilon_i}{\varepsilon_a-\varepsilon_i}<1, \quad 0<\frac{\varepsilon_a-\varepsilon_h}{\varepsilon_a-\varepsilon_i}<1, \quad 0<\frac{\varepsilon_h-\varepsilon_i}{\varepsilon_a-\varepsilon_h}, \tag{26}$$

and

$$0<\frac{\kappa_l-\kappa_i}{\kappa_a-\kappa_i}<1, \quad 0<\frac{\kappa_a-\kappa_l}{\kappa_a-\kappa_i}<1, \quad 0<\frac{\kappa_l-\kappa_i}{\kappa_a-\kappa_l}. \tag{27}$$

From Eqs. 15, 5 and 26, we have

$$0<C=\left(\frac{\varepsilon_h}{\varepsilon_a}\right)^{1/3}(1-\Phi)=\frac{\varepsilon_h-\varepsilon_i}{\varepsilon_a-\varepsilon_i}<1, \tag{28}$$

and

$$0<1-C=\frac{\varepsilon_a-\varepsilon_h}{\varepsilon_a-\varepsilon_i}<1. \tag{29}$$

From Eqs. 8, 14, 28 and 27, we have

$$0<CD=\left(\frac{\kappa_l}{\kappa_a}\right)^{1/3}(1-\Phi)=\frac{\kappa_l-\kappa_i}{\kappa_a-\kappa_i}<1, \tag{30}$$

and

$$0<1-CD=\frac{\kappa_a-\kappa_l}{\kappa_a-\kappa_i}<1. \tag{31}$$

From Eq. 16, we have

$$\varepsilon_h-\varepsilon_i=\frac{(\varepsilon_a-\varepsilon_h)C}{1-C} \quad \text{and} \quad \varepsilon_a-\varepsilon_i=\frac{\varepsilon_a-\varepsilon_h}{1-C}. \tag{32}$$

From Eq. 17, we have

$$\kappa_l-\kappa_i=\frac{(\kappa_a-\kappa_l)CD}{1-CD} \quad \text{and} \quad \kappa_a-\kappa_i=\frac{\kappa_a-\kappa_l}{1-CD}. \tag{33}$$

For the later calculation, the following transformation of an equation is derived by use of Eqs. 28, 29 and 16.

$$\frac{\varepsilon_h(\kappa_l-\kappa_a CD)}{\kappa_l(\varepsilon_h-\varepsilon_a C)}=1+\frac{\frac{\varepsilon_a}{\varepsilon_h}C-\frac{\kappa_a}{\kappa_l}CD}{1-\frac{\varepsilon_a}{\varepsilon_h}C}$$

$$=1+\frac{\varepsilon_a}{\varepsilon_i}\frac{(\varepsilon_h-\varepsilon_i)}{(\varepsilon_a-\varepsilon_h)}\frac{(D^2-1)}{D^2}. \tag{34}$$

Therefore, we can derive the following relation by use of Eqs. 21 and 34.

$$S=\left[1+\frac{C(D-1)}{1-CD}\right]\left[1+\frac{\varepsilon_a}{\varepsilon_i}\frac{(\varepsilon_h-\varepsilon_i)}{(\varepsilon_a-\varepsilon_h)}\frac{(D+1)}{D^2}(D-1)\right]. \tag{35}$$

Taking Eqs. 20 and 21 into account, we have the following relations

$$S\gtrless 1,\ D\gtrless 1 \text{ according as } \begin{cases} T>1, \text{ W/O type emulsion.} \\ T=1, \text{ homogeneous solution.} \\ T<1, \text{ O/W type emulsion.} \end{cases} \tag{36}$$

This relation 36 is transformed as

$$\frac{\kappa_i}{\varepsilon_i}\gtrless\frac{\kappa_l}{\varepsilon_h}\gtrless\frac{\kappa_a}{\varepsilon_a} \text{ according as } D\gtrless 1, \tag{37}$$

which are the part of relations 18 and 19.

4.3 Restriction with κ_l/ε_l

From Eq. 6, we have

$$\frac{\varepsilon_l}{\kappa_l}=\frac{\varepsilon_a(2\kappa_a+\kappa_i)(\kappa_l-\kappa_i)+3\varepsilon_i\kappa_a(\kappa_a-\kappa_l)}{(2\kappa_l+\kappa_i)(\kappa_a-\kappa_i)\kappa_a}. \tag{38}$$

By use of Eq. 38, we derive

$$\frac{\varepsilon_l}{\kappa_l}-\frac{\varepsilon_a}{\kappa_a}=\frac{3(\kappa_a-\kappa_l)}{(\kappa_a-\kappa_i)}\frac{\varepsilon_i\varepsilon_a}{(2\kappa_l+\kappa_i)\kappa_a}\left(\frac{\kappa_a}{\varepsilon_a}-\frac{\kappa_i}{\varepsilon_i}\right). \tag{39}$$

Therefore we have

$$\frac{\kappa_l}{\varepsilon_l}\gtrless\frac{\kappa_a}{\varepsilon_a} \text{ according as } D\gtrless 1. \tag{40}$$

4.4 Restriction with κ_h/ε_h

From Eq. 7, we have

$$\frac{\kappa_h}{\varepsilon_h}=\frac{\kappa_a(2\varepsilon_a+\varepsilon_i)(\varepsilon_h-\varepsilon_i)+3\kappa_i\varepsilon_a(\varepsilon_a-\varepsilon_h)}{(2\varepsilon_h+\varepsilon_i)(\varepsilon_a-\varepsilon_i)\varepsilon_a}. \tag{41}$$

By use of Eq. 41, we derive

$$\frac{\kappa_h}{\varepsilon_h}-\frac{\kappa_a}{\varepsilon_a}=\frac{3(\varepsilon_a-\varepsilon_h)}{(\varepsilon_a-\varepsilon_i)}\frac{\varepsilon_i}{(2\varepsilon_h+\varepsilon_i)}\left(\frac{\kappa_i}{\varepsilon_i}-\frac{\kappa_a}{\varepsilon_a}\right). \tag{42}$$

Therefore, we have

$$\frac{\kappa_h}{\varepsilon_h} \gtrless \frac{\kappa_a}{\varepsilon_a} \text{ according as } D \gtrless 1. \tag{43}$$

4.5 Relation between κ_i/ε_i and κ_h/ε_h

By use of Eq. 42, we have

$$\frac{\kappa_i}{\varepsilon_i} - \frac{\kappa_h}{\varepsilon_h} = \frac{(2\varepsilon_a+\varepsilon_i)}{(2\varepsilon_h+\varepsilon_i)} \frac{(\varepsilon_h-\varepsilon_i)}{(\varepsilon_a-\varepsilon_i)} \left(\frac{\kappa_i}{\varepsilon_i} - \frac{\kappa_a}{\varepsilon_a}\right). \tag{44}$$

Therefore, we have

$$\frac{\kappa_i}{\varepsilon_i} \gtrless \frac{\kappa_h}{\varepsilon_h} \text{ according as } D \gtrless 1. \tag{45}$$

4.6 Relation between κ_i/ε_i and κ_l/ε_l

By use of Eq. 39, we have

$$\frac{\varepsilon_i}{\kappa_i} - \frac{\varepsilon_l}{\kappa_l} = \frac{(2\kappa_a+\kappa_i)}{(2\kappa_l+\kappa_i)} \frac{(\kappa_l-\kappa_i)}{(\kappa_a-\kappa_i)} \left(\frac{\varepsilon_i}{\kappa_i} - \frac{\varepsilon_a}{\kappa_a}\right). \tag{46}$$

Therefore, we have

$$\frac{\kappa_i}{\varepsilon_i} \gtrless \frac{\kappa_l}{\varepsilon_l} \text{ according as } D \gtrless 1. \tag{47}$$

4.7 Summary of Existing Domains

From Eqs. 37, 40, 43, 45 and 47, the relative magnitude of κ_a/ε_a, κ_l/ε_l, κ_l/ε_h, κ_h/ε_h and κ_i/ε_i can be summarized as follows:
For W/O type,

$$\frac{\kappa_a}{\varepsilon_a} < \frac{\kappa_l}{\varepsilon_l} < \frac{\kappa_l}{\varepsilon_h} < \frac{\kappa_h}{\varepsilon_h} < \frac{\kappa_i}{\varepsilon_i} \text{ when } D>1,\ T>1,\ S>1. \tag{48}$$

For homogeneous solutions,

$$\frac{\kappa_a}{\varepsilon_a} = \frac{\kappa_l}{\varepsilon_l} = \frac{\kappa_l}{\varepsilon_h} = \frac{\kappa_h}{\varepsilon_h} = \frac{\kappa_i}{\varepsilon_i} \text{ when } D=1,\ T=1,\ S=1. \tag{49}$$

For O/W type,

$$\frac{\kappa_i}{\varepsilon_i} < \frac{\kappa_l}{\varepsilon_l} < \frac{\kappa_l}{\varepsilon_h} < \frac{\kappa_h}{\varepsilon_h} < \frac{\kappa_a}{\varepsilon_a} \text{ when } D<1,\ T<1,\ S<1. \tag{50}$$

These relations 48, 49 and 50 which were derived analytically are in conformity with inequality relations 18 and 19 which were understood graphically in Figs. 3 and 4.

The existing domains of κ_a/ε_a and κ_i/ε_i are illustrated in Fig. 5 for the restrictions by Eqs. 37, 40, 43, 45 and 47 and for the resultant restrictions. According to the figure, the existing domain of κ_a/ε_a is either $\kappa_a/\varepsilon_a < \kappa_l/\varepsilon_l$ or $\kappa_h/\varepsilon_h < \kappa_a/\varepsilon_a$ according as D>1 or D<1.

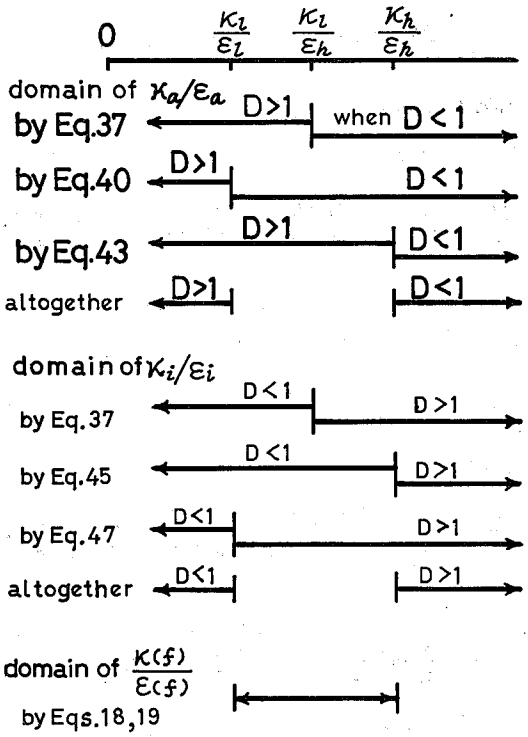

Fig. 5. Existing domains of κ_a/ε_a, κ_i/ε_i and $\kappa(f)/\varepsilon(f)$.

V. SEARCHING DIRECTION OF κ_a/ε_a TO FIND THE CORRECT ROOT OF $J(\kappa_a)=0$

Provided that ε_h, κ_l, ε_a and an approximate value of κ_a are known by experiments, a quantity D^3 is readily calculated by the relation

$$\frac{\varepsilon_a\kappa_l}{\kappa_a\varepsilon_h}=D^3, \tag{51}$$

which is identical with Eq. 14. Next, a root κ_a of $J(\kappa_a)=0$ given by Eq. 9 is searched by varying the value of κ_a. In this instance, the value of κ_a starts from $\varepsilon_a\kappa_l/\varepsilon_l$ and towards the smaller values of κ_a when $D^3>1$. When $D^3<1$, then the searching for κ_a should be proceeded from $\varepsilon_a\kappa_h/\varepsilon_h$ and towards the larger values of κ_a.

As regards the criterion of the searching direction, either T$\gtrless$1 or S$\gtrless$1 can be adopted in place of $D^3\gtrless 1$.

VI. SOME NUMERICAL EXAMPLES

In order to examine the applicability of the improved evaluation proposed above, five numerical examples are shown.

First of all, a set of phase parameters ε_a, ε_i, κ_a, κ_i and Φ was assumed. Next, the dielectric parameters ε_h, κ_l, ε_l and κ_h were calculated from Eqs. 5, 8, 6 and 7 by use of the values of ε_a, ε_i, κ_a, κ_i and Φ which were assumed above. Those values for five

Table I. Numerical Values of the Parameters in Some Examples to Test the Improved Method of Computer Searching for the Correct Root of $J(\kappa_a)=0$ Given by Eq. 9.

	Example 1	Example 2	Example 3	Example 4	Example 5
Figure shown	Fig. 6	Fig. 7	Fig. 8	Fig. 9	Fig. 10
Emulsion type	O/W	O/W	W/O	W/O	W/O
ε_a	2	80	80	2	80
ε_i	80	2	2	80	2
κ_a/μS cm^{-1}	30	100	1	1	1
κ_i/μS cm^{-1}	1	1	0.3	1000	30
Φ	0.8	0.8	0.8	0.8	0.8
ε_l	95.86	9.774	11.78	144.9	325.7
ε_h	38.27	9.729	9.729	38.27	9.729
κ_l/μS cm^{-1}	3.951	10.27	0.4035	93.42	15.53
κ_h/μS cm^{-1}	165.1	10.32	0.4586	346.6	36.85
$D^3=\frac{\varepsilon_a\kappa_l}{\kappa_a\varepsilon_h}$	0.006882	0.8447	3.318	4.882	127.7
$\varepsilon_a\frac{\kappa_l}{\varepsilon_l}/\mu$S cm^{-1}	0.08243	84.08	2.741	1.289	3.815
$\varepsilon_a\frac{\kappa_l}{\varepsilon_h}/\mu$S cm^{-1}	0.2065	84.48	3.318	4.882	127.7
$\varepsilon_a\frac{\kappa_h}{\varepsilon_h}/\mu$S cm^{-1}	8.630	84.88	3.771	18.11	303.0
$\varepsilon_a\frac{\kappa_i}{\varepsilon_i}/\mu$S cm^{-1}	0.025	40.0	12.0	25.0	1200

examples are listed in Table I together with the vaules of D^3, $\varepsilon_a\kappa_l/\varepsilon_l$, $\varepsilon_a\kappa_l/\varepsilon_h$, $\varepsilon_a\kappa_h/\varepsilon_h$ and $\varepsilon_a\kappa_i/\varepsilon_i$.

The curve of $J(\kappa_a)$ which is given by Eq. 9 as a function of κ_a is depicted in Figs. 6, 7, 8, 9 and 10. In these figures, the arrows → show the present improved searching direction (abbreviated to ISD) for the correct root (CR) of $J(\kappa_a)=0$ following the new evaluation proposed above.

In the previous paper, a scheme of the primitive searching direction (PSD) for the correct root of $J(\kappa_a)=0$ was suggested as follows:

(i) If $\kappa_a<\kappa_l<\kappa_i$, then the value of κ_a starts from κ_l for smaller values of κ_a.

(ii) If $\kappa_a>\kappa_l>\kappa_i$, then the value of κ_a starts from κ_l for larger values of κ_a.

These primitive searching directions are shown with double arrows →→ in the figures.

Example 1 (Fig. 6)

Both the improved searching direction (ISD) → and the primitive searching direction (PSD) →→ attain the correct root (CR) of $J(\kappa_a)=0$ straightway.

Example 2 (Fig. 7)

The primitive searching starts from κ_l for larger values of κ_a (the right direction), and meets with an unidentified false root (UFR) and a point for $D=1$. Afterwards the searching attains the correct root.

The improved searching starts from $\varepsilon_a\kappa_h/\varepsilon_h$ for larger values of κ_a, and attains the correct root straightway.

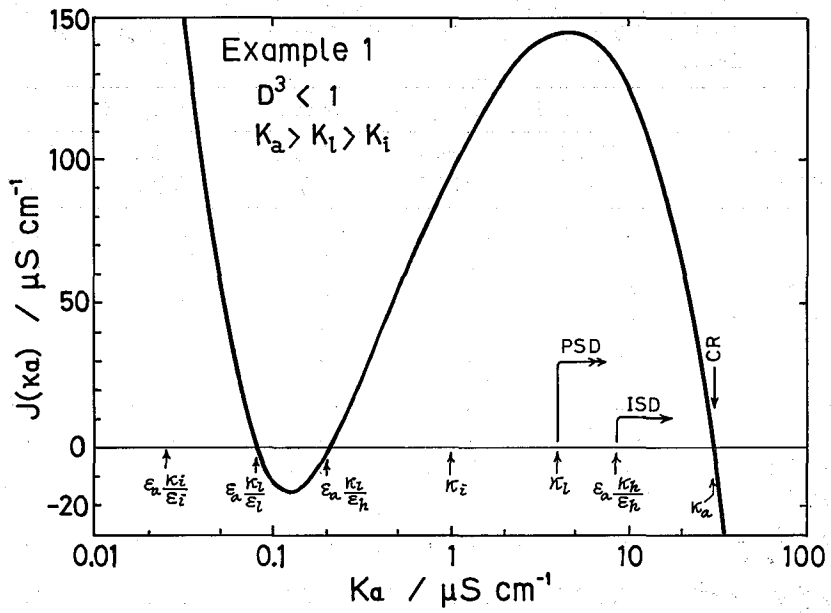

Fig. 6. The curve of the function $J(\kappa_a)$ given by Eq. 9 against κ_a for Example 1. In the figure, PSD with a double arrow ↠ means the primitive searching direction, and ISD with an arrow → denotes the improved searching direction. An abbreviation CR shows the location of the correct root of $J(\kappa_a)=0$. The numerical values of the parameters used are listed in Table I.

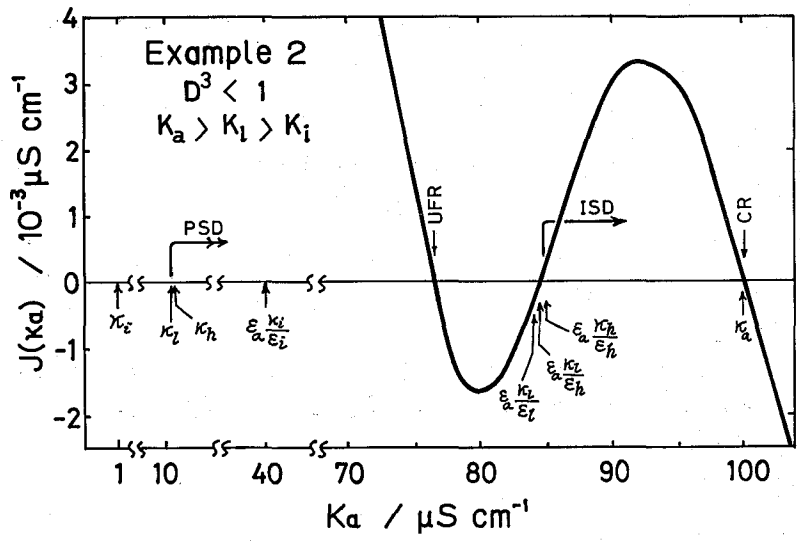

Fig. 7. The curve of the function $J(\kappa_a)$ given by Eq. 9 against κ_a for Example 2.

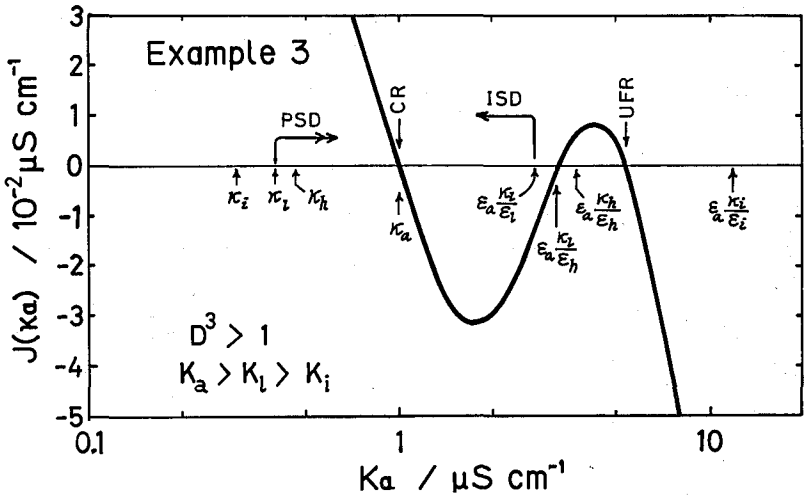

Fig. 8. The curve of the function $J(\kappa_a)$ given by Eq. 9 against κ_a for Example 3.

Example 3 (Fig. 8)

The primitive searching starts from κ_l for the right direction, attaining the correct root.

The improved searching starts from $\varepsilon_a\kappa_l/\varepsilon_l$ for the left direction, attaning the correct root.

Exampie 4 (Fig. 9)

The primitive searching starts from κ_l for the left direction, and meets with an unidentified false root (UFR) and a point for D=1. This unidentified false root gives a set of plausible values: $\Phi=0.6602$, $\varepsilon_i=400.7$ and $\kappa_i=176.0$ μS cm^{-1}. The farther searching attains the correct root.

The improved searching starts from $\varepsilon_a\kappa_l/\varepsilon_l$ for the left direction, and attains the correct root straightway.

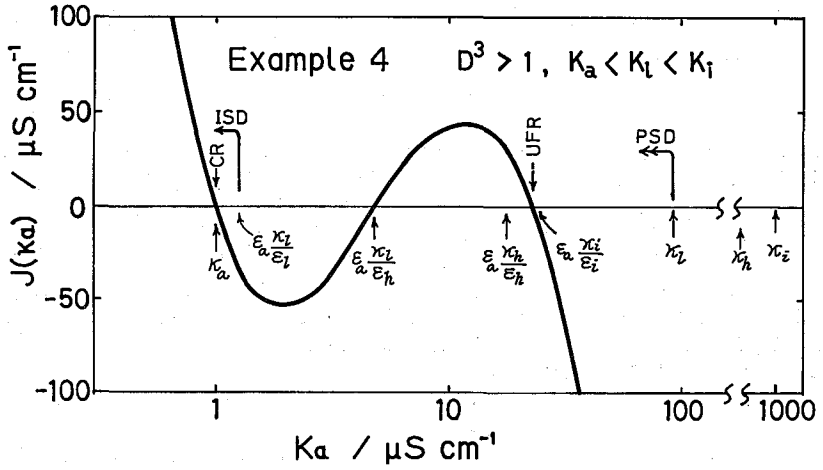

Fig. 9. The curve of the function $J(\kappa_a)$ given by Eq. 9 against κ_a for Example 4.

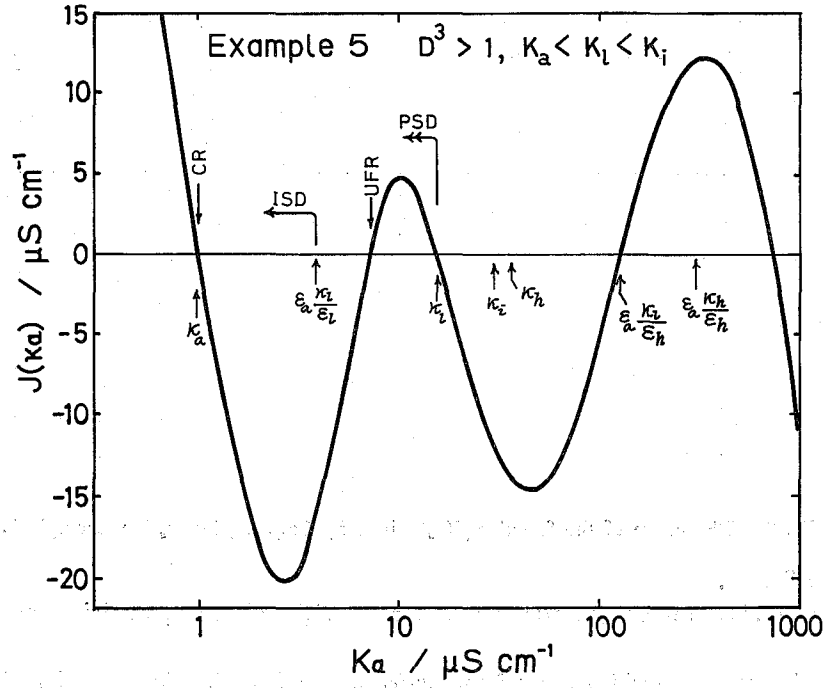

Fig. 10. The curve of the function $J(\kappa_a)$ given by Eq. 9 against κ_a for Example 5.

Example 5 (Fig. 10)

The primitive searching starts from κ_l for the left direction, and meets with an unidentified false root (UFR). This unidentified false root gives a set of unrealistic values: $\phi = 0.129$, $\varepsilon_i = -43.6$ and $\kappa_i = -56.2$ μS cm^{-1}. Afterwards the searching sttains the correct root.

The improved searching starts from $\varepsilon_a \kappa_l / \varepsilon_l$ for the left direction, and attains the correct root straightway.

It is concluded that the improved searching always attains the correct root without meeting with the false roots in contrast with the primitive searching scheme which often meets with false roots.

REFERENCES

(1) L. K. H. van Beek, Dielectric behaviour of Heterogeneous Systems, in "Progress in Dielectrics," Vol. 7 ed. by J. B. Birks, Heywood Books, London, 1967, pp. 69-114.
(2) T. Hanai, Electrical Properties of Emulsions, in "Emulsion Science," Chapter 5, ed. by P. Sherman, Academic Press, London and New York, 1968, pp. 353-478.
(3) S. S. Dukhin, Dielectric Properties of Disperse Systems, in "Surface and Colloid Science," Vol. 3, ed. by Egon Matijević, Wiley-Interscience, New York and London, 1971, pp. 83-165.
(4) J. C. Maxwell, "A Treatise on Electricity and Magnetism," Third ed., Vol. I, Chap. IV, Art. 310-314, Clarendon Press, Oxford, (1891), pp. 435-441.
(5) K. W. Wagner, *Arch. Electrotech.*, **2**, 371 (1914).
(6) T. Hanai, *Kolloid Z.*, **171**, 23 (1960).
(7) T. Hanai, *Kolloid Z.*, **175**, 61 (1961).
(8) T. Hanai, A. Ishikawa and N. Koizumi, *Bull. Inst. Chem. Res., Kyoto Univ.*, **55**, 376 (1977).